Serna Merino, PM.; Rodríguez-Fernández, A.; Yacob, S.; Kliewer, C.; Moliner Marin, M.; Corma Canós, A. (2021). Single-Site vs. Cluster Catalysis in High Temperature Oxidations. Angewandte Chemie International Edition. 60(29):15954-15962. https://doi.org/10.1002/anie.202102339

Single-Site vs Cluster Catalysis in High Temperature Oxidations

Pedro Serna,[a]* Aida Rodríguez-Fernández,[b] Sara Yacob,[a] Christine Kliewer,[a] Manuel Moliner,[b]* Avelino Corma[b]*

[a] Dr. P. Serna, Dr. S. Yacob, Dr. C. Kliewer
ExxonMobil Research and Engineering Co., Corporate Strategic Research, Annandale, New Jersey 08801, United States
[b] A. Rodríguez-Fernández, Dr. M. Moliner, Prof. A. Corma
Instituto de Tecnología Química, Universitat Politècnica de València - Consejo Superior de Investigaciones Cientificas (UPV-CSIC), Av. de los Naranjos, s/n, 46022 Valencia, Spain
E-mails: pedro.m.serna-merino@exxonmobil.com, mmoliner@itq.upv.es, acorma@itq.upv.es

Supporting information for this article is given via a link at the end of the document.

Abstract: The behavior of single Pt atoms and small Pt clusters for high temperature oxidation reactions has been investigated using CHA zeolite, denoting that subtle changes in the atomic structure of the active sites are responsible for drastic changes in performance driven by specific metal-ligand interactions between the metal, the gas-phase components, and the support — in our case, a well-defined, non-reducible macro-ligand. The high-stability of these molecular sites inside CHA, without direct contributions by the support into the evaluated redox chemistry, is a key to more intrinsic structure-performance descriptions in elemental reaction steps such as O_2 dissociation, and the subsequent catalysis in reactions of industrial interest, such as the combustion of methane, propane, and CO. Interestingly, whereas single Pt-atoms and Pt nanoparticles larger than, approximately, 1 nm are unable to activate, scramble and desorb two O_2 molecules in isotopic exchange experiments at moderate temperature (i.e. 200ºC), clusters smaller than 1 nm can do so catalytically, despite being unstable against oxidative fragmentation at these temperatures, leading to catalyst deactivation. For oxidative processes that require the activation of rather inert molecules at a high temperature, like alkanes, catalytic combustion is attributed to stable single Pt atoms when the support is CHA, which are generated *in situ* in the O_2 stream even if the sample has been pre-reduced in H_2 to start from zero-valent metal clusters. The alkane combustion activity is facilitated when the reacting alkane, acting as a reductant, includes weaker C-H bonds (e.g. propane vs methane). The C-H cleavage is inferred to be the rate-determining reaction step, which is less sensitive to changes in the size of the active site compared to the effects observed in the O_2 scrambling experiments. When the combustion catalysis engages a strong reductant such as CO, instead of the alkane, the catalysis appears to be dominated by metal clusters and nanoparticles, and not single Pt atoms, as the latter are incapable of forming a stable mononuclear carbonyl species inside the zeolite. The great stability of both single Pt atoms in the combustion of methane, and of small Pt clusters in the combustion of CO, including upon regeneration and/or steaming, open new opportunities for the system in a variety of high temperature oxidation scenarios.

Introduction

Highly-dispersed transition metal catalysts are extensively used in chemical and petrochemical processes.[1] Their catalytic properties are determined by the exact nature of the active species, which often varies over time in response to temperature and interaction with fluid phase components.[1,2] Noble metal catalysts, in particular, tend to undergo permanent deactivation by irreversible sintering when exposed to severe redox and hydrothermal stress.[1,3] Many research efforts have been devoted in recent years to improve the stability of well-dispersed transition metals under relevant industrial conditions, which is most problematic when the actives sites are isolated metal atoms and clusters of a few atoms.[4–6] Those active sites have drawn significant attention by the scientific community over the last decade,[1,5,7–9] since they can offer opportunities that more conventional metal ensembles like nanoparticles or bulk phases do not.[10,11] To help to stabilize the metal, a second more robust sub-structure, called the support, is typically introduced to serve as a solid dispersion media and an active site diluent, while introducing mechanical strength and favorable mass and heat transfer.[5,6]

Keeping metal active sites stable is particularly challenging in processes that require high temperature and/or pressure, and go through alternating oxidative and reductive conditions (e.g. reaction vs regeneration), which favor metal agglomeration. Moreover, catalysts may destabilize at different moments of their lifetime for different reasons, corresponding to different mechanisms of activity loss under variable conditions. This requires researchers to address multiple facets of the problem through a single material. For example, the coalescence of noble metals by Brownian motion typically dominates in H_2 streams (e.g. during pre-activation steps or in hydrogenation/dehydrogenation reactions), whereas Ostwald-ripening via single-atom intermediates is usually favored in O_2 (e.g. during coke burn out operations);[3,12] and for temperatures greater than ~400°C, volatile MeO_x species may also form, which must be trapped before they start contributing to the sintering problem by incorporation to other distant metal particles.[3,13]

Among the supports, zeolites can be adequate thanks to their high stability, high surface area, porous nature, and the possibility to build multifunctional catalysis.[14–20] Moreover, zeolites are well-defined crystalline, tunable supports that can play analog roles to ligands in organometallic and biological systems, while helping to stabilize isolated metal atoms and clusters.[19,21–25] Several recent publications have emphasized the dynamic nature of molecular metal sites inside zeolites using operando characterization techniques, showing that they may participate in complex cyclic processes of cluster formation and cluster re-dispersion in contact with the gas phase components.[18,26–28]

Recently, we have described the stabilization of several metals (Pt, Pd, and bimetallic PtPd) within the cavities of highly siliceous CHA zeolite, under severe redox stress (i.e. at temperatures as high as 650°C, in both H_2 and O_2, and steam).[21,29] These materials offer three important advantages for their use as heterogeneous catalysts: (1) high hydrothermal stability; (2)

shape-selectivity, to discriminate molecules smaller and larger than ~4 Å; and (3) fine-tuning of the metal speciation, from single atoms to small clusters (i.e. ~1 nm). The versatility of the metal-CHA system is unusual and allows to perform remarkably well in different industrial scenarios.

In this paper, we will show how to take advantage of the properties of highly-siliceous Pt-CHA as an efficient and robust heterogeneous oxidation catalyst. High temperature oxidation by single-site Pt and by few-atom Pt clusters remains to a large extent elusive due to the difficulty to sustain a significant population of these active sites under such a harsh chemical environment, unless the support also brings redox characteristics (i.e. on reducible supports), which complicates the disentanglement of the exact role of the supported metal vs the support itself. Thus, we have evaluated here the intrinsic behavior of single Pt atoms and small Pt clusters as oxidation species using a non-reducible support like the CHA zeolite, in where we can stabilize metal clusters and metal atoms.[21,29] Among the reactions investigated here, we include the elemental O_2 dissociation via $^{16}O_2/^{18}O_2$ isotopic exchange, and reactions with relevant industrial substrates such as methane, propane, and CO. Our work stresses the importance to build structure-performance relationships that account for subtle changes in the active sites under reaction conditions. Understanding these dynamic processes for high-temperature oxidation catalysts is necessary to identify the true active species, a step forward in the development of accurate descriptors and predictive tools for catalyst optimization.

Results and Discussion

Single Site vs Small cluster catalysis – O_2 Dissociation Experiments

Previous work by Gates et al. illustrates the effect that a single metal-metal bond can exert on (hydrogenation) catalysis.[23,30–32] A single Rh-Rh bond in MgO-supported Rh dimers, for example, is responsible for ~60 times activity boost in ethylene hydrogenation when compared to single Rh atoms, due to the improvement in the rate of H_2 dissociation.[32] Interestingly, the effect is much less pronounced when the metal sits on an electron-withdrawing support such as HY zeolite, because then the resultant electron-deficient single Rh atoms activate H_2 more effectively, making the role of the metal-metal bond secondary.[31] However, for reactions that take place at high temperatures, single noble metal atoms are generally unstable (and, thus, more difficult to evaluate) as the metal/support interaction weakens sufficiently to allow surface metal migration. Nevertheless, at moderate temperatures, usually below 100°C in H_2, mobility can be limited by judicious choice of the gas phase reactants to form stable complexes during the catalysis. This is the case, for example, of supported Rh, Ir and Ru complexes on HY or MgO for alkene hydrogenation or dimerization reactions, where stable $M(C_2H_4)_2$ species can be formed.[33] For higher temperatures, researchers must typically introduce more strongly interacting supports such as TiO_2 or CeO_2 to avoid that the molecular species sinter.[3,34] These reducible supports, however, often bring additional effects like co-activation of the reactants at the metal-support interface,[35,36] or the supply of new redox active sites[37] that obscure the evaluation and understanding of the intrinsic properties of the supported metal species. Nevertheless, we can evaluate nuclearity effects in Pt catalysts (single site vs cluster) for high temperature oxidation catalysis using CHA zeolite as a non-reducible support. This work builds on our previous observation that highly siliceous CHA can stabilize small Pt clusters of 0.8-1.5 nm in reducing H_2 streams ($Pt/CHA_{H2\text{-}400C}$, clusters comprising 10 to 150 atoms), but forms single Pt atoms in O_2 that are stable at temperatures as high as 650°C ($Pt/CHA_{O2\text{-}650C}$).[21,29]

In a first series of experiments, we have tested the performance of Pt/CHA for the dissociation of O_2 using $^{16}O_2/^{18}O_2$ isotopic exchange experiments. A mass-spectrometer was used to track the evolution of the $m_z^+ = 34$ fragment, characteristic of scrambled $^{16}O^{18}O$ that can be used as a marker for O_2 dissociation of two molecules (and subsequent desorption of the exchanged product). In these flow-through experiments, the reduced $Pt/CHA_{H2\text{-}400C}$ catalyst delivered significant amounts of $m_z^+ = 34$ at 200°C (Figure 1), whereas the oxidized $Pt/CHA_{O2\text{-}650C}$ sample barely produced scrambled O_2 above the blank signal (Figure 1). The first appearance of O_2 scrambling with the oxidized catalyst was not observed until the temperature reached ~340°C, and it was necessary to reach ~400°C before the intensity of $m_z^+ = 34$ compared to that of the pre-reduced $Pt/CHA_{H2\text{-}400C}$. We hypothesize that the absence of neighboring metal sites in the O_2-treated Pt/CHA is responsible for the lower activity to split the O–O bond, in agreement with other recent works on Pd,[38] and Pt.[39]

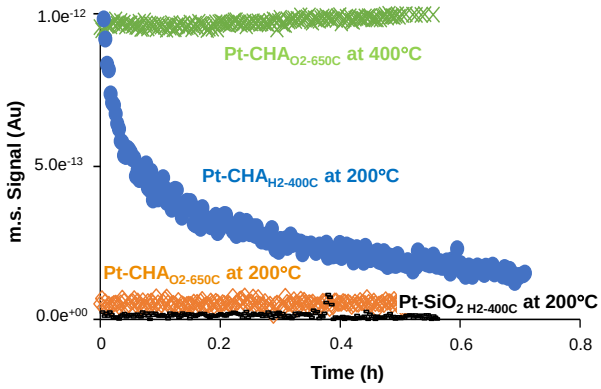

Figure 1. TOS mass spectrometry signals of $m_z^+ = 34$ during flow-through $^{16}O_2/^{18}O_2$ exchange experiments using (A) CHA-supported single Pt atoms at 200°C (orange diamonds); (B) CHA-supported single Pt atoms at 400°C (green crosses); (C) CHA-supported 0.8-1.5 nm Pt clusters at 200°C (blue circles); (D) SiO_2-supported 1.5-2 nm Pt nanoparticles at 200°C (black lines).

However, the activity of the oxidized $Pt/CHA_{O2\text{-}650C}$ sample for $^{16}O_2/^{18}O_2$ isotopic exchange remained constant over >1.5 h during the exchange experiment at 400°C (Figure S1), whereas the activity of the reduced version at 200°C continued to drop over the same period until the $m_z^+=34$ signal became almost indistinguishable from zero ($Pt/CHA_{O2—650C}$ at 200°C in Figure 1). This result shares some similarities with the work recently reported by the Cargnello's group on Pd/Al_2O_3, where it was inferred that PdO nanoparticles deactivate during methane combustion experiments due to a re-dispersion of the metal oxide phase into (inactive) single Pd atoms.[38] We observe a similar deactivation pattern with the reduced $Pt/CHA_{H2\text{-}400C}$ in the isotopic O_2 stream at 200°C, but a more detailed analysis of EXAFS data taken during this process reveals that a significant fraction of the

Pt remains as small clusters in these conditions, with a drop in the average Pt-Pt coordination number from ~ 7 to ~ 4 (Table S1).[29] The decrease in the number of Pt-Pt bonds is accompanied by a growth of Pt-O bonds without the appearance of new long-distance heavy backscatters signals, which allows us to rule out the formation of Pt-O-Pt ensembles. STEM images of the reduced $Pt/CHA_{H2\text{-}400C}$ catalyst after 2 h in O_2 at 200°C further confirm the presence of nanoparticles in the 1-1.5 nm range (Figure 2B). Indeed, to accomplish complete re-dispersion of these 1-1.5 nm Pt clusters, temperatures greater than 450°C must be employed (Table S1).[29] By combination of EXAFS and time-resolved HAADF-STEM images, we also showed that only the smallest Pt clusters (below ~1 nm) re-disperse into single Pt atoms when the conditions are relatively mild.[29] Thus, the deactivation mechanism previously proposed for alumina-supported PdO nanoparticles in methane combustion experiments [38] is insufficient to explain the complete loss of catalytic activity of the reduced Pt/CHA sample in our O_2 scrambling experiments. We note, however, that the temperature used by the Cargnello's group in their methane combustion work (775°C) is sufficiently high to cause full re-dispersion of the metal according to our previous data for Pd,[21] which supports their conclusions.

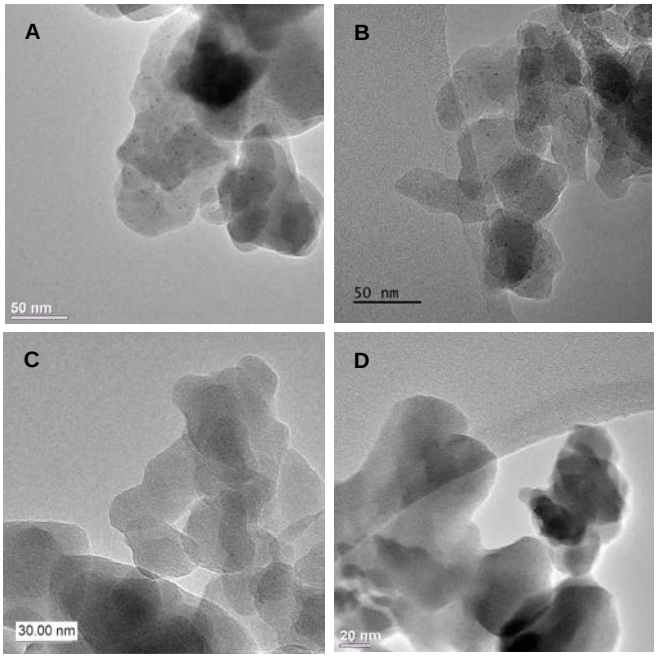

Figure 2. TEM image of a Pt/CHA sample after: (A) reduction in H_2 at 400ºC for 2 h ($Pt/CHA_{H2\text{-}400C}$); (B) reduction in H_2 at 400ºC for 2 h followed by reaction with 50 sccm of 2%O_2 in N_2 at 200ºC for 1.5 h; (C) reduction in H_2 at 400ºC for 2 h followed by reaction with 50 sccm of 2%O_2 in N_2 at 500ºC for 1.5 h; (D) reduction in H_2 at 400ºC for 2 h followed by reaction with 40 sccm of N_2, 100 sccm of 10%O_2 in N_2, and 3 sccm of 100% CH_4 at 650ºC for 24 h.

At this point, we postulated two possibilities to understand the deactivation kinetics of the reduced $Pt/CHA_{H2\text{-}400C}$ in the $^{16}O_2/^{18}O_2$ stream (Figure 1): a) at 200°C, the $^{16}O_2/^{18}O_2$ scramble only happens on Pt clusters smaller than approximately 1 nm, which are unstable and gradually form inactive single Pt atoms (in this scenario, any co-existing Pt clusters > 1 nm is postulated inactive to catalyze $^{16}O_2/^{18}O_2$ scrambling); or b) two independent deactivation phenomena are taking place—one that turns small, active Pt clusters into inactive Pt single atoms and, additionally, one by which the slightly larger Pt clusters (i.e. > 1nm) are initially active but somehow passivate over time in the presence of the O_2.

Table 1. $^{16}O_2/^{18}O_2$ isotopic exchange experiments[a] using various Pt-containing catalysts.

Entry	Sample[b]	Reaction Temperature (ºC)	m_z^+=34 Signal (a.u.)[c]
1	$Pt/CHA_{H2\text{-}400C}$	200	100-8[d]
2	$Pt/CHA_{H2\text{-}400C}$	400	95[e]
3	$Pt/CHA_{O2\text{-}650C}$	200	7.2[e]
4	$Pt/CHA_{O2\text{-}650C}$	400	97[e]
5	$Pt/SiO_{2\ H2\text{-}400C}$	200	3.4[e]
6	$Pt/SiO_{2\ H2\text{-}400C}$	400	760[e]
7	$K\text{-}Pt\text{-}MFI_{H2\text{-}400C}$	200	660-0

[a] Feed composition: 1%$^{16}O_2$, 1%$^{18}O_2$, 98% N_2
[b] WHSV = 1.5 h^{-1} for 0.4 wt % Pt/CHA; 3 h^{-1} for 0.8 wt % Pt/SiO_2; and 4 h^{-1} for 0.4 wt % K-Pt-MFI
[c] Mass spectrometer signal after background subtraction
[d] The first number corresponds to the signal at zero TOS, and the second after 60 min
[e] Mass-spectrometer signals reported 30 min after reaching the temperature setpoint, for which the m_z^+=34 signal was shown virtually steady; experiments at 400ºC were performed following O_2-scrambling at 200ºC without any other thermal treatment in between, typically, using a 5ºC/min temperature ramp.

To distinguish between these possibilities, we synthesized a third catalyst, consisting of ~1.5 to 3 nm Pt nanoparticles supported on SiO_2 (Figure S2). This system is an ideal benchmark because 1) it lacks subnanometric metal clusters and single atoms due to the weakly interacting nature of the silica support; 2) it avoids large Pt nanoparticles when properly prepared;[40] and 3) it is stable in O_2 up to approximately 400°C, as demonstrated by H_2 chemisorption experiments. Interestingly, when the reduced Pt/SiO_2 catalyst was exposed to the $^{16}O_2/^{18}O_2$ mixture at 200°C, as in the experiments conducted with the reduced $Pt/CHA_{H2\text{-}400C}$ catalyst, no isotopic exchange was observed at all ($Pt/SiO_{2\ H2\text{-}400C}$ at 200°C in Figure 1). The temperature had to be raised to ~300°C to detect the m_z^+ = 34 fragment above blank levels. At 400°C, a constant, intense signal was obtained, qualitatively superior to that of single Pt atoms in CHA (entry 6 in Table 1). The lack of any activity or deactivation profile at 200°C constitutes a strong proof that clusters >1 nm cannot close a single turnover during O_2 activation, and that the deactivation profile of the reduced $Pt/CHA_{H2\text{-}400C}$ in Figure 1 is not the result of a gradual surface passivation. Abrupt deactivation is, indeed, a more likely scenario for these systems following O_2 dissociation. O_2 dissociation is anticipated to occur on Pt surfaces with a rather low-energy barrier.[41] We infer, thus, that the lack of $^{16}O_2/^{18}O_2$ exchange activity on the Pt/SiO_2 likely responds to the formation of oxygen adatoms too strongly bounded to the catalyst surface after the first O_2 dissociation event. These inferences hold reasonable for the $Pt/CHA_{O2\text{-}650C}$ sample, based on CO oxidation literature that suggest that single Pt atoms can dissociate O_2,[42,43] with a notable difference that the activation of two oxidizing molecules in $^{16}O_2/^{18}O_2$ scramble experiments is probably hindered when each site only brings one metal center. In contrast, the observation that $Pt/CHA_{H2\text{-}400C}$ is

active, but unstable over a rather long period of time (>1h) under otherwise identical reaction conditions, unambiguously demonstrates that there is a second, more gradual, deactivation mechanism due to sites that are present in the Pt/CHA catalyst, but not in Pt/SiO_2. This leads us to postulate that subnanometric Pt clusters in Pt/CHA are the only contributing species to the $^{16}O_2/^{18}O_2$ exchange activity in Figure 1, with both single Pt atoms and larger Pt nanoparticles acting as mere spectators (at least when the temperature is moderate, i.e. 200°C). We find remarkable that single Pt atoms and >1 nm Pt clusters show a similar onset reaction temperature (300-400°C) despite the obvious differences in their nature/structure, while clusters <1 nm, structurally in between, are much more active.

Why/how the smallest metal clusters are able to scramble $^{16}O_2/^{18}O_2$ at a rather low temperature remains unclear, but we were able to demonstrate that the scrambling process is not stoichiometric, but catalytic (i.e. that more than one turnover per Pt atom is attainable). Interestingly, while so far we have been unable to sustain catalytic $^{16}O_2/^{18}O_2$ scrambling activity at a temperature as low as 200°C, we managed to significantly increase the amount of $^{16}O^{18}O$ produced during our exchange experiments by increasing the amount of initial subnanometric Pt active sites in the catalyst. This objective was accomplished by rational selection of K-Pt-MFI as the O_2-scrambling catalyst, which we recently showed contains most of the Pt in the form of <0.8 nm clusters.[19] Then, a notably higher initial concentration of $m_z^+ = 34$ was observed in our experiment, despite a similar decay in activity over time as with the Pt/CHA sample (Table 1, Entry 7). We postulate that oxidative fragmentation is also responsible for the loss of activity over time in this case (currently under investigation) but, in any case, we can determine that 0.058 mmol of O_2 were scrambled over 0.012 mmol of Pt in the reactor at the end of the process, which is unambiguously indicative of catalysis. On the other hand, the data demonstrate that catalytic $^{16}O_2/^{18}O_2$ scrambling also happens on the $Pt/CHA_{O2\text{-}650C}$ sample, characterized by the lack of Pt-Pt bonds according to EXAFS (within the experimental error), provided that the temperature is high enough (stable $m_z^+ = 34$ signal at 400°C, Figure 1, and Figure S1).

We see plausible that the Al sites of the zeolite, or any other source of negative charge from the zeolite framework, like defects generated when alkali elements where added to the synthesis gel,[19] may be playing some role in these processes, especially when the reaction temperature is high (e.g. > 400°C). As we and others have suggested,[21,44] the Al sites in CHA are the most likely grafting points to stabilize single Pt or Pd atoms. This observation is rather common in instances where the extra-framework species are cationic, for example in Cu dimers and trimers,[27,45] and single atoms of noble metals under specific synthesis and reaction conditions.[5] Before reaching the Al site, PtO_x species generated by oxidation of zero-valent clusters in the starting $Pt/CHA_{H2\text{-}400C}$ sample would be travelling through either the gas-phase, if the temperature is high enough,[21] or through charge-neutral regions of the zeolite. In any of these two scenarios, the landing of PtO_x onto a surface site that is negatively charged at the Al position would be expected to cause weakening of the Pt-O bonds, and the promotion of O_2 desorption (or $^{16}O^{18}O$) upon recombination. We think that this process probably requires the participation of a pair of adjacent Al sites of the zeolite framework, similar to what has been reported for other transition metals like Cu,[27,28,46] which is consistent with our previous observation that Pt in CHA sinters in O_2 at high temperature, instead of stabilizing as single atoms, when the Si/Al ratio is too high.[21] Interestingly, whether the single Pt sites end grafted to Al pairs previously counterbalanced by Na^+ or H^+, or both, remains unclear, but our mass spectrometer data allow to rule out the formation of water concomitantly to the release of $^{16}O^{18}O$ (Figure S3). Although the mechanism of metal migration and stabilization inside CHA is not be fully understood, recent investigations show via Density Functional Theory that the preference of Pt single atoms growth inside zeolites can be kinetically hindered by the proper density of suitable rings, Si:Al ratio, and the loading of Pt atoms.[47]

Single Site vs Small cluster catalysis – Methane and propane oxidation experiments

A catalyst initially containing single Pt atoms in CHA (i.e. $Pt/CHA_{O2\text{-}650C}$) was contacted with a mixture of $O_2/CH_4/N_2$ at increasing temperatures. First evidences of CO_2 formation were observed in the 435 to 475°C temperature range (Figure 3), thereby slightly higher than the temperature at which O_2 isotopic exchange was observed with this catalyst (~340°C). These results suggest that the combustion of methane is not limited by the O_2 dissociation step but, likely, the C–H cleavage. The intrinsic behavior of single Pt atoms in oxidation catalysis has remained elusive due to the difficulty to stabilize and investigate these isolated species at high temperatures on supports that lack redox functionality (it has been otherwise reported for reducible supports, which help to stabilize the single metal atoms, but also have a direct contribution to the catalysis).[48] To gather more information about the alkane activation process, we performed additional combustion experiments with the $Pt/CHA_{O2\text{-}650C}$ sample using propane as the reacting hydrocarbon, which includes weaker C–H bonds compared to methane. Propane reacted in the presence of O_2 and the single-atom Pt species at 200-300°C (entry 3 in Table 2), with almost quantitative conversion of the limiting reagent at 300°C. These temperatures are notably lower than those needed to combust methane in Figure 3 (435°C), and lower than the temperature needed to scramble oxygen in the $^{16}O_2/^{18}O_2$ exchange experiments (~340°C). These data is indeed consistent with a situation where the C–H cleavage in CH_4 is the rate determining step.

On the other hand, the pre-reduced $Pt/CHA_{H2\text{-}400C}$, with small 0.8-1.5 nm metal clusters, combusts propane in a similar temperature range (Table 2). We acknowledge that a fraction of the initial Pt-Pt bonds in this sample may breakup under the oxidizing propane combustion environment, but we expect the majority of the metal to remain as small clusters/nanoparticles taking into account that a) the T in this experiment is rather low; and b) the propane/O_2 ratio is rather high (1:1). As a reference, we previously reported that the Pt-Pt coordination number of $Pt/CHA_{H2\text{-}400C}$ decays from ~7 to ~4 at 200°C when the gas contains diluted O_2 and no hydrocarbon (i.e. no reductant) is present (Table S1).[29] Consistent with these observations, Pt/SiO_2, consisting of ~2 nm Pt nanoparticles, also starts reacting propane at ~200°C and consumes the O_2 almost quantitatively at 300°C (entry 8 in Table 2). This series of experiments is important, because it indicates that despite notable differences in the way O_2 is activated by single Pt atoms and Pt clusters (Figure 1 and Table 1), the active site nuclearity less of an effect on the C–H activation, which is the key elemental step in these oxidation processes, as rate-determining. The data provided in this paper does not allow, however, to rule out some degree of metal nuclearity effects in the

C-H activation process, which have been otherwise extensively reported for the activation of alkanes like methane at high temperatures.[49–51] The fact that propane reacts below the temperature at which the $^{16}O_2/^{18}O_2$ scrambling occurs suggests, moreover, that O_2 dissociation does indeed take place in all these cases, but it is likely followed by irreversible formation of rather strong Pt–O bonds that are only broken at low temperatures (i.e. < 250°C) if a relatively strong reductant is present.

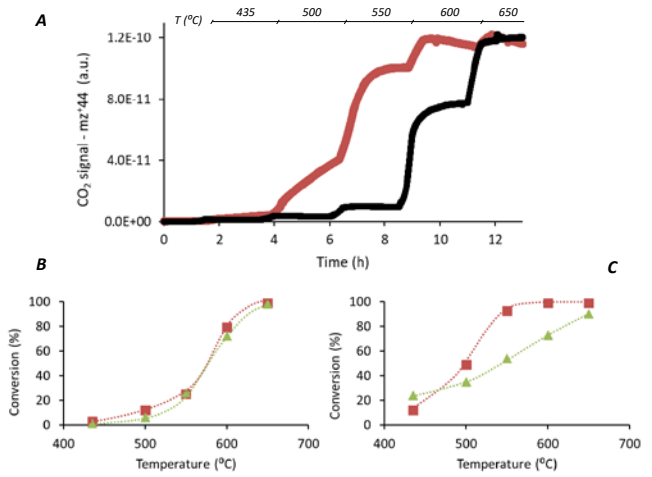

Figure 3. CH_4 combustion using Pt/CHA and Pd/CHA pretreated in O_2 at 650ºC: (A) mass spectrometry signal for fragment 44 (CO_2) as the temperature is raised in the 435-650°C range stepwise (soak time was 2 h for all steps, excepts for the highest temperature, which was 24 h in the case of the $Pt/CHA_{O2\text{-}650C}$, and 6 h in the case of $Pd/CHA_{O2\text{-}650C}$); (B) and (C) are the corresponding methane conversion data at the end of each step, as the temperature was ramped up (red curve) and then ramped down (green curve) after the 650ºC aging step (24 h for Pt, and 6 h for Pd); Reaction conditions: 71 mg of 0.4 wt % Pt/CHA or 142 mg of 0.2 wt % Pd/CHA; Feed = 40 sccm N_2, 100 sccm 10%O_2 in N_2, 3 sccm 100%CH_4

Remarkably, the differences in reactivity between $Pt/CHA_{O2\text{-}650C}$ and $Pt/CHA_{H2\text{-}400C}$, manifested in both O_2 scrambling and propane combustion experiments, are no longer observed when the reacting hydrocarbon is methane and the temperature must be raised > 500°C to achieve some meaningful conversion (e.g. 10 % of the limiting reagent, Table 2). Under the harsher oxidizing conditions for methane combustion (higher T and higher O_2/hydrocarbon ratio of 3:1), one should expect that both $Pt/CHA_{O2\text{-}650C}$ and $Pt/CHA_{H2\text{-}400C}$ mainly consist of single Pt atoms, considering that oxidative fragmentation of Pt clusters in CHA is virtually completed at 500°C in diluted O_2, as evidenced by EXAFS in Table S1. This inference was further supported by comparison of STEM images of a fresh and a spent $Pt/CHA_{H2\text{-}400C}$ catalyst after the CH_4 combustion experiment, which shows the disappearance of any feature attributable to Pt-Pt nanoparticles or clusters (Figure 2D).

The methane combustion activity of single Pt atoms in CHA is lower than that of the best oxidation catalysts reported in the literature, such as supported PdO nanoparticles.[39] The differences between Pt and Pd as a combustion catalyst is widely discussed in previous reports,[52–54] and here we put the accent in the performance of single metal atoms to activate both O_2 and the hydrocarbon. The Pt/CHA system is particularly suitable for this purpose because it is structurally simpler and more stable at high temperature in O_2 compared to other catalysts, as discussed next.

Figure 3A shows the evolution of CO_2 measured by mass spectrometry at the outlet of the reactor, as the T is ramped stepwise from 435°C to 650°C in an O_2-rich O_2/CH_4 stream. At each step, the soak time was 2 h before ramping to the next temperature, except for the highest T, which was held for 24 h (not shown). After 24 h at 650°C, the experiment was run backwards to collect data at decreasing temperatures from 650°C to 435°C. Figure 3B shows the approximate methane conversion at each temperature, both during the ramp up and ramp down experiments.

Table 2. Combustion of methane and propane with Pt-catalysts

Entry	Sample[b]	Pt loading (wt%)	Substrate[a]	mg Cat	React. Temp. (°C)	Conv.[b] (%)
1	$Pt/CHA_{H2\text{-}400C}$	0.4	Meth.	71	300	0
2	$Pt/CHA_{H2\text{-}400C}$	0.4	Meth.	71	500	12
3	$Pt/CHA_{O2\text{-}650C}$	0.2	Prop.	9.4	200	0.7[c]
4	$Pt/CHA_{O2\text{-}650C}$	0.2	Prop.	9.4	300	15.8[c]
5	$Pt/CHA_{H2\text{-}400C}$	0.2	Prop.	10	200	0.9[c]
6	$Pt/CHA_{H2\text{-}400C}$	0.2	Prop.	10	300	18.0[c]
7	$Pt/SiO_{2\ H2\text{-}400C}$	0.8	Prop.	4.8	200	0.8[c]
8	$Pt/SiO_{2\ H2\text{-}400C}$	0.8	Prop.	4.8	300	17.9[c]

[a] Feed composition: For methane: 40 sccm N_2, 100 sccm 10%O_2 in N_2, 3 sccm 100%CH_4; for propane: 0.5 sccm Ar, 5 sccm O_2, 5 sccm propane, 89.5 sccm He
[b] Hydrocarbon conversion
[c] The conversion of the limiting reagent (O_2) is ~5 times the conversion of the hydrocarbon

The stability of $Pt/CHA_{O2\text{-}650C}$ after 24 h at 650°C is remarkable (Figure 3B), in a stream that contains O_2, CH_4, CO_2 and H_2O (in variable amounts at the inlet and outlet of the reactor, corresponding to changes in conversion from 0 to 100 %, respectively). The rate of CO_2 formation at each temperature appears to be fairly constant over the 2 h period investigated, and the activity reported on the ramp up and ramp down are virtually identical. This scenario contrasts with that observed on a Pd/CHA counterpart, more active when fresh as evidenced by a lower onset reaction temperature, but manifesting complex activation and deactivation processes on stream (activity continuously going up at constant T for T < 500°C, but continuously going down for T > 500°C, Figures 3A and 3C). This result is independent of the treatment used to activate the Pd/CHA catalyst, to initiate the reaction with either 1-2 nm particles (reductive pre-treatment) or single Pd atoms (oxidizing pre-treatment). The non-steady phenomena at each temperature step complicates drawing straightforward structure/performance correlations. Our STEM data on the spent Pd/CHA catalysts show that the majority of the CHA crystals lack metal structures visible under the electron beam, although some areas show rather large Pd aggregates (Figure S4). We hypothesize that the deactivation observed at the highest temperatures (>550°C) responds to the fragmentation of active PdO_x clusters into less active single Pd atoms, similar to the results reported by the Cargnello group on Pd/Al_2O_3.[38] This re-dispersion phenomenon probably outcompetes other activation events (unresolved, but likely related to formation of

PdO particles) that may occur at lower T, evidenced by the increasing conversion at constant T (T<500°C, red curve, Figure 3A).

Single Site vs Small cluster catalysis – CO oxidation

Our data above show that, in CHA zeolite, O_2 can re-disperse < 1 nm Pt clusters and 1-2 nm Pt clusters at 200°C and ~ 500°C, respectively, during alkane combustion experiments.

Next, we show that this situation is notably different when Pt/CHA is used for the oxidation of an even stronger reductant such as CO, which is another very relevant substrate in petrochemical and automotive industries. The results we present here show once more how important is to understand the influence of gas/solid interactions to shape the catalyst structure under working conditions.[26]

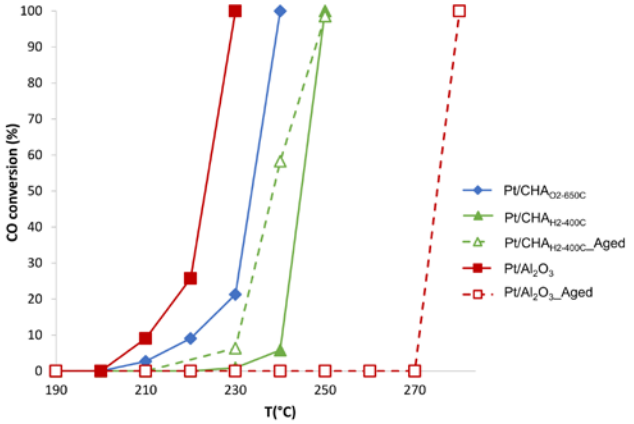

Figure 4. CO conversion at different T using Pt/CHA$_{O2-650C}$, Pt/CHA$_{H2-400C}$ and Pt/Al_2O_3 catalysts in their fresh forms (filled) and after being aged (empty). The ageing treatments were: air at 750°C for 13 h followed by H_2 at 400°C for 2 h for the Pt/CHA$_{H2-400C}$ sample, and air at 750°C for 13 h for Pt/Al_2O_3.

The CO oxidation activity of Pt/CHA was tested with the catalyst pre-treated in O_2 at 650°C (Pt/CHA$_{O2-650C}$) or H_2 at 400°C (Pt/CHA$_{H2-400C}$). For comparison purposes, we also tested a reference sample, in this case Pt/Al_2O_3 because it is the most universal industrial benchmark. The Pt/Al_2O_3 catalyst was made by incipient wetness impregnation of Pt$(NH_3)(NO_3)_2$ on γ-alumina to deliver well-dispersed ~2nm Pt particles upon activation in H_2 at 400°C.

Figure 4 shows the light off curves for the combustion of CO using these three catalysts under O_2-rich reaction conditions (O_2/CO=6.3). The onset CO oxidation temperature for the fresh catalysts (solid lines) follows the order Pt/Al_2O_3 > Pt/CHA$_{O2-650C}$ > Pt/CHA$_{H2-400C}$. Full conversion of the CO occurs in the 230 to 250°C range for all the catalysts. The T required to combust CO is notably lower than that needed to activate CH_4, consistent with the more inert nature of the latter (stronger bonds). However, we found surprising that Pt/CHA$_{O2-650C}$ (with single Pt atoms) and Pt/CHA$_{H2-400C}$ (with 0.8-1.5 nm particles), behaved so similar. To better understand these results, we characterized the spent catalysts using STEM, and the presence of metal nanoparticles in all cases is observed (Figure 5). We conclude, thus, that CO promotes the consolidation of Pt-Pt bonds, through a process that outcompetes the effect of O_2 as a re-dispersing agent. Said that, we still note some remarkable differences between the various samples depending on the activation treatment. For example, while Pt/CHA$_{O2-650C}$, initially containing single Pt atoms, sinters in the CO stream to yield relatively larger particles (some of them >4 nm, and clearly outside the CHA crystals), the pre-reduced Pt/CHA$_{H2-400C}$ sample holds 1-2 nm particles under otherwise identical conditions (Figure 5).

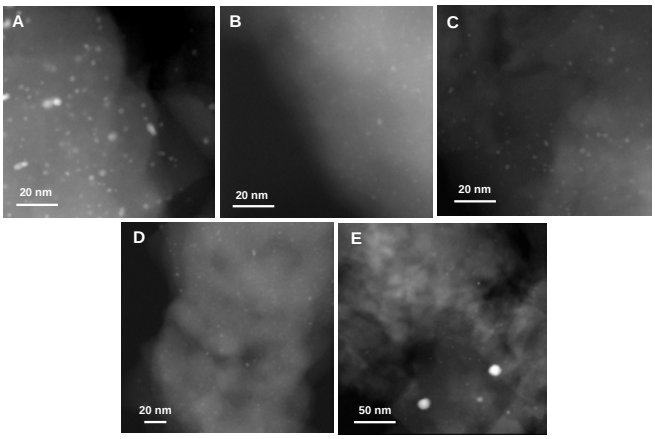

Figure 5. STEM images of Pt/CHA$_{O2-650C}$ (a), Pt/CHA$_{H2-400C}$ (b) and Pt/Al_2O_3 (c) catalysts after CO oxidation, and STEM images of Pt/CHA$_{H2-400C}$ (d) and Pt/Al_2O_3 (e) after ageing treatments and CO oxidation reaction. The ageing treatments were: air at 750°C for 13 h followed by H_2 at 400°C for 2 h for the Pt/CHA$_{H2-400C}$ sample, and air at 750°C for 13 hours for the Pt/Al_2O_3 sample.

The role of CO as a metal structure modifier is not easy to anticipate. CO can be regarded as both an effective reductant [55–57] and an effective oxidant,[16,31] and literature often invokes either argument to explain the experimental observations. CO has been proved to cause sintering or re-dispersion of different supported metal species depending on a number of factors that can be hard to rationalize. On the one hand, CO adds oxidatively to metal surfaces and complexes in the absence of any other chemical event, as other ligands like hydrogen or alkenes do.[58] On small zero-valent metal clusters of Rh and Ir, CO can even cause oxidative fragmentation to single (cationic) *gem*-dicarbonyl complexes on supports like DAY zeolite, MgO or Al_2O_3.[16,31,59] In these processes, reaction of M-CO fragments with –OH groups of the support facilitate oxidation of the metal and the adsorption of a second CO molecule.[59] On the other hand, CO can facilitate reduction of the active sites, which usually occurs if any of the following situations apply: a) the metal surface is covered by labile (reactive) oxygen, which is eliminated as CO_2 upon reaction with the CO; or b) the oxidative addition of CO to the metal results in unstable M-CO species that continue to migrate onto the support until a new more stable metallic cluster or nanoparticle is formed. The latter can be avoided, for example, by using a support able to trap the migrating carbonyl fragments, as in the case of Rh/DAY, where *gem*-dicarbonyl Rh$(CO)_2$ species become ultra-stabilized at the Al sites of the zeolite.[60] It is worth noting that although H_2 also adds oxidatively to metals, the result of treating single metal atoms of, for example, Rh with H_2 is typically a site with more reduced metal centers, because hydride-containing Rh single sites are relatively unstable and bond too weakly to the support to restrict their surface migration and subsequent particle growth. In these cases, Brownian motion usually stops at a given T when the particle reaches a threshold size that provides sufficient metal-

support bonding. The presence of additional ligands bonded to the metal further complicates these types of analyses.[60]

Our work here evidences that single Pt atoms in $Pt/CHA_{O2\text{-}650C}$ do not form stable small carbonyl fragments or complexes in CO, but rather large nanoparticles outside the zeolite crystals (Figure 5). In this aggregation process, collisions inside the zeolite between carbonyl-carrying Pt ensembles and –OH groups of the support are likely to occur, but we postulate their product to be rather unstable or, otherwise, no metal would accumulate at the external surface of the zeolite. Our data indicates that this scenario is avoided, however, if sufficiently large Pt ensembles are intentionally generated inside the zeolite prior to exposure to the CO stream, as in $Pt/CHA_{H2\text{-}400C}$, which remain virtually unchanged after the interaction with CO (Figure 5). These 1-2 nm Pt clusters inside CHA resist, thus, any oxidative (re-dispersing) attack by the CO under the conditions investigated.

On the other hand, many CO oxidation applications require that the metal stays stable after exposed to particularly extreme conditions, for example in diesel engines.[61–63] To simulate similar conditions, we tested the light off performance of the benchmark Pt/Al_2O_3 and the $Pt/CHA_{H2\text{-}400C}$ after they had been subjected to an extra aging step in air at 750°C for 13 h before the catalytic test. Due to the severity of this treatment, the onset reaction temperature of the benchmark Pt/Al_2O_3 sample shifted from 210°C to >270°C (Figure 4). This shift was accompanied by clear symptoms of metal sintering in the corresponding STEM images, showing the formation of Pt agglomerates larger than ~20 nm (Figure 5). This result is consistent with previous literature.[12,13] The aggregation is ascribed to the occurrence of Ostwald ripening of volatile PtO_x arising from the small Pt nanoparticles that are trapped by larger (more stable) ones, resulting in an overall particle growth.[12,64] As we previously reported,[21,29] the CHA framework is an excellent atom-trapping support under identical conditions, eliminating this hard-to-prevent sintering problem. Accordingly, the performance of the aged Pt/CHA catalyst, activated in H_2 prior to the CO oxidation reaction, is nearly identical to the one observed with the unaged catalyst, as the particle size distribution inferred from the STEM images remains virtually the same (see Figure 5). This catalyst, thus, is not only stable, but more active than the Pt/Al_2O_3 benchmark after a single aging step, which is also an important result from a more practical standpoint.

Conclusions

The dynamic behavior of single Pt atoms and small Pt clusters trapped within a non-reducible support such as CHA zeolite has been studied during oxidation reactions to elucidate structure-performance relationships following subtle changes in the active sites under working conditions. Our findings demonstrate that clusters <1 nm are more active than single atoms and >1 nm clusters to dissociate, recombine and desorb O_2; and that the exact nature of the working species depends on complex interactions between the gas-phase components, the metal species and the support that can be largely understood thanks to the excellent properties of CHA to trap and stabilize rather uniform, small metal species under the harsh reaction conditions investigated. Oxidative fragmentation of most active < 1 nm clusters into single Pt atoms is shown responsible for the gradual loss of isotopic $^{16}O_2/^{18}O_2$ exchange activity at moderate T (i.e. 200ºC). In the case of methane combustion, negligible catalytic differences were observed for samples initially containing either single Pt or small Pt clusters, as temperatures above 500°C are needed to achieve any meaningful CH_4 conversion, for which single metal atoms are formed in either case, as demonstrated by *in situ* EXAFS spectroscopy and *ex situ* STEM microscopy. First evidences of CO_2 formation on single Pt atoms occur at a T higher than that required for isotopic O_2 scrambling when the substrate is methane, but not when it is propane, suggesting that these combustion processes by single atoms are not limited by O_2 dissociation, but C–H activation. And, interestingly, our experiments suggest that the O_2 scrambling activity is more sensitive to changes in the active site nuclearity than the activation of C–H bonds in propane, as combustion of the later occurs at fairly low temperatures on both single Pt atoms and small Pt nanoparticles. Pt in CHA, on the other hand, stabilizes as small metal clusters during processes that involve the presence of CO, and leads to high activity and improved stability compared to reference Pt/Al_2O_3 formulations.

Experimental Section

Experimental information on synthesis, characterization and testing of catalysts are given in the SI.

Acknowledgements

This work has been supported by the Spanish Government through SEV-2016-0683 and RTI2018-101033-B-I00 (MCIU/AEI/FEDER, UE). The Electron Microscopy Service of the UPV is acknowledged for their help in sample characterization. A.R.F. acknowledges the Spanish Government-MINECO for a FPU scholarship (FPU2017/01521). We thank Isabel Millet, Tom Green and Michael Caulfield for technical assistance and to Randall Meyer for his comments and additional discussions when writing this paper. We appreciate the support of ExxonMobil Research and Engineering for our efforts in fundamental catalytic research.

Keywords: Zeolite • single-site • metal cluster • oxidation catalyst • structure-activity relationship

References

[1] L. Liu, A. Corma, *Chem. Rev.* **2018**, *118*, 4981–5079.
[2] L. Liu, A. Corma, *Nat. Rev. Mater.* **2020**, DOI 10.1038/s41578-020-00250-3.
[3] J. Jones, H. Xiong, A. T. DeLaRiva, E. J. Peterson, H. Pham, S. R. Challa, G. Qi, S. Oh, M. H. Wiebenga, X. I. Pereira Hernandez, Y. Wang, A. K. Datye, *Science* **2016**, *353*, 150–154.
[4] X. Cui, W. Li, P. Ryabchuk, K. Junge, M. Beller, *Nat. Catal.* **2018**, *1*, 385–397.
[5] B. C. Gates, M. Flytzani-Stephanopoulos, D. A. Dixon, A. Katz, *Catal. Sci. Technol.* **2017**, *7*, 4259–4275.
[6] B. C. Gates, *Trends Chem.* **2019**, *1*, 99–110.
[7] K. Narsimhan, K. Iyoki, K. Dinh, Y. Román-Leshkov, *ACS Cent. Sci.* **2016**, *2*, 424–429.
[8] A. Wang, J. Li, T. Zhang, *Nat. Rev. Chem.* **2018**, *2*, 65–81.
[9] J. D. A. Pelletier, J.-M. Basset, *Acc. Chem. Res.* **2016**, *49*, 664–677.
[10] S. Vajda, M. J. Pellin, J. P. Greeley, C. L. Marshall, L. A. Curtiss, G. A. Ballentine, J. W. Elam, S. Catillon-Mucherie, P. C. Redfern, F. Mehmood, P. Zapol, *Nat. Mater.* **2009**, *8*, 213–216.
[11] G. Kwon, G. A. Ferguson, C. J. Heard, E. C. Tyo, C. Yin, J.

DeBartolo, S. Seifert, R. E. Winans, A. J. Kropf, J. Greeley, R. L. Johnston, L. A. Curtiss, M. J. Pellin, S. Vajda, *ACS Nano* **2013**, *7*, 5808–5817.
[12] T. W. Hansen, A. T. DeLaRiva, S. R. Challa, A. K. Datye, *Acc. Chem. Res.* **2013**, *46*, 1720–1730.
[13] S. B. Simonsen, I. Chorkendorff, S. Dahl, M. Skoglundh, J. Sehested, S. Helveg, *J. Am. Chem. Soc.* **2010**, *132*, 7968–7975.
[14] N. Wang, Q. Sun, R. Bai, X. Li, G. Guo, J. Yu, *J. Am. Chem. Soc.* **2016**, *138*, 7484–7487.
[15] L. Liu, U. Díaz, R. Arenal, G. Agostini, P. Concepción, A. Corma, *Nat. Mater.* **2017**, *16*, 132–138.
[16] J. Zhang, L. Wang, B. Zhang, H. Zhao, U. Kolb, Y. Zhu, L. Liu, Y. Han, G. Wang, C. Wang, D. S. Su, B. C. Gates, F.-S. Xiao, *Nat. Catal.* **2018**, *1*, 540–546.
[17] S. Goel, S. I. Zones, E. Iglesia, *J. Am. Chem. Soc.* **2014**, *136*, 15280–15290.
[18] P. Serna, B. C. Gates, *J. Am. Chem. Soc.* **2011**, *133*, 4714–4717.
[19] L. Liu, M. Lopez-Haro, C. W. Lopes, C. Li, P. Concepcion, L. Simonelli, J. J. Calvino, A. Corma, *Nat. Mater.* **2019**, *18*, 866–873.
[20] K. H. Rasmussen, J. Mielby, S. Kegnæs, *ChemCatChem* **2018**, *10*, 4380–4385.
[21] M. Moliner, J. Gabay, C. Kliewer, P. Serna, A. Corma, *ACS Catal.* **2018**, *8*, 9520–9528.
[22] P. W. Kletnieks, A. J. Liang, R. Craciun, J. O. Ehresmann, D. M. Marcus, V. A. Bhirud, M. M. Klaric, M. J. Hayman, D. R. Guenther, O. P. Bagatchenko, D. A. Dixon, B. C. Gates, J. F. Haw, *Chem. - A Eur. J.* **2007**, *13*, 7294–7304.
[23] P. Serna, B. C. Gates, *Acc. Chem. Res.* **2014**, *47*, 2612–2620.
[24] Q. Sun, N. Wang, Q. Bing, R. Si, J. Liu, R. Bai, P. Zhang, M. Jia, J. Yu, *Chem* **2017**, *3*, 477–493.
[25] L. Liu, M. Lopez-Haro, D. M. Meira, P. Concepcion, J. J. Calvino, A. Corma, *Angew. Chemie Int. Ed.* **2020**, *59*, 15695–15702.
[26] L. Liu, D. N. Zakharov, R. Arenal, P. Concepcion, E. A. Stach, A. Corma, *Nat. Commun.* **2018**, *9*, 574.
[27] C. Paolucci, I. Khurana, A. A. Parekh, S. Li, A. J. Shih, H. Li, J. R. Di Iorio, J. D. Albarracin-Caballero, A. Yezerets, J. T. Miller, W. N. Delgass, F. H. Ribeiro, W. F. Schneider, R. Gounder, *Science* **2017**, *357*, 898–903.
[28] K. T. Dinh, M. M. Sullivan, K. Narsimhan, P. Serna, R. J. Meyer, M. Dincă, Y. Román-Leshkov, *J. Am. Chem. Soc.* **2019**, *141*, 11641–11650.
[29] M. Moliner, J. E. Gabay, C. E. Kliewer, R. T. Carr, J. Guzman, G. L. Casty, P. Serna, A. Corma, *J. Am. Chem. Soc.* **2016**, *138*, 15743–15750.
[30] C. Aydin, J. Lu, N. D. Browning, B. C. Gates, *Angew. Chemie Int. Ed.* **2012**, *51*, 5929–5934.
[31] J. Lu, P. Serna, C. Aydin, N. D. Browning, B. C. Gates, *J. Am. Chem. Soc.* **2011**, *133*, 16186–16195.
[32] D. Yardimci, P. Serna, B. C. Gates, *Chem. - A Eur. J.* **2013**, *19*, 1235–1245.
[33] P. Serna, B. C. Gates, *Angew. Chemie Int. Ed.* **2011**, *50*, 5528–5531.
[34] Y. Tang, C. Asokan, M. Xu, G. W. Graham, X. Pan, P. Christopher, J. Li, P. Sautet, *Nat. Commun.* **2019**, *10*, 4488.
[35] A. Corma, P. Serna, *Science* **2006**, *313*, 332–334.
[36] A. Corma, P. Serna, P. Concepción, J. J. Calvino, *J. Am. Chem. Soc.* **2008**, *130*, 8748–8753.
[37] S. Carrettin, P. Concepción, A. Corma, J. M. López Nieto, V. F. Puntes, *Angew. Chemie Int. Ed.* **2004**, *43*, 2538–2540.
[38] E. D. Goodman, A. C. Johnston-Peck, E. M. Dietze, C. J. Wrasman, A. S. Hoffman, F. Abild-Pedersen, S. R. Bare, P. N. Plessow, M. Cargnello, *Nat. Catal.* **2019**, *2*, 748–755.
[39] B. Nan, X.-C. Hu, X. Wang, C.-J. Jia, C. Ma, M.-X. Li, R. Si, *J. Phys. Chem. C* **2017**, *121*, 25805–25817.
[40] S. Soled, *Science* **2015**, *350*, 1171–1172.
[41] P. D. Nolan, B. R. Lutz, P. L. Tanaka, J. E. Davis, C. B. Mullins, *J. Chem. Phys.* **1999**, *111*, 3696–3704.
[42] B. Qiao, A. Wang, X. Yang, L. F. Allard, Z. Jiang, Y. Cui, J. Liu, J. Li, T. Zhang, *Nat. Chem.* **2011**, *3*, 634–641.
[43] T. Kropp, Z. Lu, Z. Li, Y.-H. C. Chin, M. Mavrikakis, *ACS Catal.* **2019**, *9*, 1595–1604.
[44] J. Van der Mynsbrugge, M. Head-Gordon, A. T. Bell, *J. Mater. Chem. A* **2021**, DOI 10.1039/D0TA11254B.
[45] S. Grundner, M. A. C. Markovits, G. Li, M. Tromp, E. A. Pidko, E. J. M. Hensen, A. Jentys, M. Sanchez-Sanchez, J. A. Lercher, *Nat. Commun.* **2015**, *6*, 7546.
[46] J. R. Di Iorio, R. Gounder, *Chem. Mater.* **2016**, *28*, 2236–2247.
[47] D. Hou, L. Grajciar, P. Nachtigall, C. J. Heard, *ACS Catal.* **2020**, *10*, 11057–11068.
[48] J. Guzman, S. Carrettin, A. Corma, *J. Am. Chem. Soc.* **2005**, *127*, 3286–3287.
[49] J. Wei, E. Iglesia, *J. Catal.* **2004**, *224*, 370–383.
[50] G. Jones, J. Jakobsen, S. Shim, J. Kleis, M. Andersson, J. Rossmeisl, F. Abildpedersen, T. Bligaard, S. Helveg, B. Hinnemann, *J. Catal.* **2008**, *259*, 147–160.
[51] Y. Wang, L. Xiao, Y. Qi, J. Yang, Y.-A. Zhu, D. Chen, *J. Phys. Chem. C* **2020**, *124*, 2501–2512.
[52] E. D. Goodman, S. Dai, A.-C. Yang, C. J. Wrasman, A. Gallo, S. R. Bare, A. S. Hoffman, T. F. Jaramillo, G. W. Graham, X. Pan, M. Cargnello, *ACS Catal.* **2017**, *7*, 4372–4380.
[53] H. Nie, J. Y. Howe, P. T. Lachkov, Y.-H. C. Chin, *ACS Catal.* **2019**, *9*, 5445–5461.
[54] W. Qi, J. Ran, R. Wang, X. Du, J. Shi, J. Niu, P. Zhang, M. Ran, *RSC Adv.* **2016**, *6*, 109834–109845.
[55] Y. Kang, X. Ye, C. B. Murray, *Angew. Chemie* **2010**, *122*, 6292–6295.
[56] G. Chen, Y. Tan, B. Wu, G. Fu, N. Zheng, *Chem. Commun.* **2012**, *48*, 2758.
[57] Y. Dai, X. Mu, Y. Tan, K. Lin, Z. Yang, N. Zheng, G. Fu, *J. Am. Chem. Soc.* **2012**, *134*, 7073–7080.
[58] J. A. Labinger, *Organometallics* **2015**, *34*, 4784–4795.
[59] A. Suzuki, Y. Inada, A. Yamaguchi, T. Chihara, M. Yuasa, M. Nomura, Y. Iwasawa, *Angew. Chemie Int. Ed.* **2003**, *42*, 4795–4799.
[60] P. Serna, D. Yardimci, J. D. Kistler, B. C. Gates, *Phys. Chem. Chem. Phys.* **2014**, *16*, 1262–1270.
[61] A. S. Ivanova, E. M. Slavinskaya, R. V. Gulyaev, V. I. Zaikovskii, O. A. Stonkus, I. G. Danilova, L. M. Plyasova, I. A. Polukhina, A. I. Boronin, *Appl. Catal. B Environ.* **2010**, *97*, 57–71.
[62] Y. Xie, E. Rodrigues, N. Furtado, A. Matynia, T. Arlt, P. Rodatz, P. Da Costa, *Top. Catal.* **2016**, *59*, 1039–1043.
[63] M. H. Wiebenga, C. H. Kim, S. J. Schmieg, S. H. Oh, D. B. Brown, D. H. Kim, J.-H. Lee, C. H. F. Peden, *Catal. Today* **2012**, *184*, 197–204.
[64] T. R. Johns, R. S. Goeke, V. Ashbacher, P. C. Thüne, J. W. Niemantsverdriet, B. Kiefer, C. H. Kim, M. P. Balogh, A. K. Datye, *J. Catal.* **2015**, *328*, 151–164.

Entry for the Table of Contents

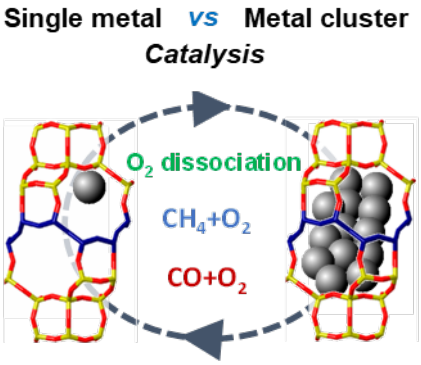

Metal active sites speciation on Pt-CHA is discussed for different high-temperature oxidation reactions, including $^{16}O_2/^{18}O_2$isotopic exchange experiments, methane combustion and CO oxidation, unraveling structure-performance relationships built on subtle changes in the active sites under working conditions